Yu *et al. Arthritis Research & Therapy* (2024) 26:185
https://doi.org/10.1186/s13075-024-03422-6

Arthritis Research & Therapy

RESEARCH Open Access

Circ-CAMTA1 regulated by Ca^{2+} influx inhibited pyruvate carboxylase activity and modulate T cell function in patients with systemic lupus erythematosus

Hui-Chun Yu[1], Hsien-Yu Huang Tseng[1], Hsien-Bin Huang[2] and Ming-Chi Lu[1,3*]

Abstract

Objectives To investigate the roles of Ca^{2+} influx-regulated circular RNAs (circRNAs) in T cells from patients with systemic lupus erythematosus (SLE).

Methods The expression profile of circRNAs in Jurkat cells, co-cultured with and without ionomycin, was analyzed by next-generation sequencing and validated using real-time polymerase chain reaction. The identified Ca^{2+} influx-regulated circRNAs were further examined in T cells from 42 patients with SLE and 23 healthy controls. The biological function of specific circRNA was investigated using transfection and RNA pull-down assay.

Results After validation, we confirmed that the expression levels of circ-ERCC4, circ-NFATC2, circ-MYH10, circ-CAMTA1, circ-ASH1L, circ-SOCS7, and circ-ASAP1 were consistently increased in Jurkat cells following Ca^{2+} influx. The expression levels of circ-CAMTA1, circ-ASH1L, and circ-ASAP1 were significantly lower in T cells from patients with SLE, with even lower levels observed in those with higher disease activity. Interferon (IFN)-α was found to suppress the expression of circ-CAMTA1. Circ-CAMTA1 bound to pyruvate carboxylase and inhibited its biological activity. Overexpression of circ-CAMTA1, but not its linear form, significantly decreased extracellular glucose levels. Furthermore, increased expression of circ-CAMTA1, but not its linear form, decreased miR-181c-5p expression, resulting increased IL-2 secretion.

Conclusion Three Ca^{2+} influx-regulated circ-RNAs—circ-CAMTA1, circ-ASH1L, and circ-ASAP1 —were significantly reduced in T cells from patients with SLE and associated with disease activity. IFN-α suppressed the expression of circ-CAMTA1, which interacted with pyruvate carboxylase, inhibited its activity, affected glucose metabolism, and increased IL-2 secretion. These findings suggest that circ-CAMTA1 regulated by Ca^{2+} influx modulated T cell function in patients with SLE.

Keywords Circular RNAs, Ca^{2+} influx, Systemic lupus erythematosus, T cells, Disease activity, Pyruvate carboxylase

*Correspondence:
Ming-Chi Lu
e360187@yahoo.com.tw
[1]Division of Allergy, Immunology and Rheumatology, Dalin Tzu Chi Hospital, Buddhist Tzu Chi Medical Foundation, No. 2, Minsheng Road, Dalin, Chiayi 62247, Taiwan
[2]Department of Life Science, Institute of Molecular Biology, National Chung Cheng University, Minxiong, Chiayi, Taiwan
[3]School of Medicine, Tzu Chi University, Hualien City, Taiwan

Introduction

Systemic lupus erythematosus (SLE) is a chronic systemic autoimmune disease characterized by a wide range of clinical manifestations with a highly variable relapsing-remitting course. The disease predominantly affects women of reproductive age. The pathogenesis of SLE is highly complex, involving genetic inheritance, environmental factors, and hormonal influences, which collectively lead to dysregulation of both the innate and adaptive immune system [1]. T cells play a critical role in immune regulation, and multiple T cell dysfunction, including aberrant cytokine secretion, disrupted cell signal transduction, and altered metabolism, have been observed in patients with SLE [2]. Among these mechanisms, increased and prolonged Ca^{2+} influx in SLE T cells following stimulation activates calmodulin kinases, calcineurin, and the nuclear factor of activated T cells (NFAT) pathway, resulting in decreased interleukin (IL)-2 secretion were well documented [3–5]. The most important is that voclosporin, a novel calcineurin inhibitor targeting the Ca^{2+} signaling pathway, was approved for the treatment of SLE recently [6].

Noncoding RNAs (ncRNAs) are functional RNA molecules transcribed from DNA but not translated into proteins. They are conventionally classified into long ncRNAs (lncRNAs) and short ncRNAs (sncRNAs), based on whether they are more than or less than 200 nucleotides in length [7]. LncRNAs can be further categorized into subclasses based on their different properties, with the most common being long intergenic ncRNAs (lincRNAs), antisense RNAs (asRNAs), pseudogenes, and circular RNAs (circRNAs) [8]. Our previous studies have demonstrated aberrant expression of lncRNAs in T cells from patients with rheumatoid arthritis (RA) and ankylosing spondylitis (AS) participated inflammatory responses [9, 10]. Among the lncRNAs, circRNAs are synthesized through the back-splicing of pre-mRNA transcripts and the back-splicing junction sequence of circRNAs is crucial for their identification. The lack of free ends renders circRNAs highly stable, and makes them becoming a new and important research focus [11]. CircRNAs can regulated gene expression by acting as miRNA sponges, interacting with proteins or occasionally directly translating proteins. Thus, circRNAs have numerous biological functions and are involved in the pathophysiology of various immune diseases [12].

In a review article, Wang et al. summarized that several circRNAs have been showed to be differentially expressed in peripheral blood mononuclear cells (PBMCs) or plasma from patients with SLE compared to those of the controls [13]. Aberrant expression of circRNAs has been implicated in the immunopathogenesis of SLE [14]. However, few studies have investigated the potential aberrantly expressed circRNAs in SLE T cells and their roles in the immunopathogenesis of SLE. For instance, Li et al. demonstrated that SLE T cells had lower expression levels of hsa_circ_0045272, negatively regulating T-cell apoptosis and IL-2 secretion [15]. Zhang et al. showed that downregulation of hsa_circ_0012919 could increase the expression of DNMT1, reduce the expression of CD70 and CD11, and regulate KLF13 and RANTES through miR-125a binding [16]. CircPTPN22 (hsa_circ_0110529), downregulated in the PBMCs from patients with SLE, has been found to increase proliferation and inhibit apoptosis in Jurkat cells [17]. Given the complex immunopathogenesis of SLE, we believe that additional circRNAs contributing to the pathogenesis of SLE can be identified in SLE T cells. Our previous study also demonstrated that Ca^{2+} influx regulates the expression of miRNAs in Jurkat cells and overexpression of miR-524-5p increased IFN-γ production in activated T cells [18]. We hypothesized that Ca^{2+} influx can regulate the expression of circRNAs in T cells and that these Ca^{2+} influx-regulated circRNAs are aberrantly expressed in T cells from patients with SLE, contributing to T cell dysfunction, including altered cytokine secretion, cell activation, signaling pathway, and metabolic process in SLE.

Materials and methods

Cell culture

To identify Ca^{2+} influx-regulated circRNAs, Jurkat cells (American Type Culture Collection, Manassas, VA, USA) were cultured with or without 1 μg /mL ionomycin (Sigma-Aldrich, St. Louis, MO, USA) for 1 h at 37°C in a humidified atmosphere containing 5% CO_2. To analyzed circRNA expression levels in Jurkat cells after stimulation, cells were treated with phorbol 12-myristate 13-acetate (PMA; 20 ng/mL; Sigma-Aldrich) and ionomycin (500 ng/mL; Sigma-Aldrich,) for 24 h. For analysis of circRNA expression in response to interferon-alpha (IFN-α), Jurkat cells were treated with 1000 IU/mL recombinant human IFN-α for 72 h. The IFN-alpha we used was purchased from Proteintech (Rosemont, IL, USA) and was produced in HEK293. Subsequently, the cells were harvested for further analysis. The cell-free supernatants were collected by centrifugation at 300 x g for 10 min and were stored at -80℃ until analysis.

Patients and controls

Forty-two patients aged 20 years and older with a clinician-confirmed diagnosis of SLE according to the 1997 American College of Rheumatology (ACR) revised criteria [19] or the 2012 Systemic Lupus International Collaborating Clinics (SLICC) Classification Criteria [20] were recruited. Twenty-three age- and sex-matched healthy volunteers were enrolled as a control group. All the participants signed informed consent under a study protocol approved by the institutional review board of Dalin Tzu

Chi Hospital, Buddhist Tzu Chi Medical Foundation (No. B11003006). The study was performed in accordance with the Declaration of Helsinki. Demographic data of the SLE patients and controls were recorded, and SLE disease activity was assessed using the Systemic Lupus Erythematosus Disease Activity Index 2000 (SLEDAI-2K) [21]. Blood samples were collected at least 12 h after the last dose of immunosuppressants to minimize drug effects.

Isolation of RNA from T cells

PBMCs were isolated from heparinized venous blood using the dextran sedimentation method described in our earlier study [22]. T cells were further purified using anti-human CD3 magnetic beads by IMag Cell Separation System (BD Bioscience, Franklin Lakes, USA). Total RNA from the T cells was extracted using the TRIZOL kit (Invitrogen, Carlsbad, CA, USA) according to the manufacturer's protocol. The RNA concentration was quantified using a NanoDrop Spectrophotometer. For the measurement of circRNAs, purified RNA was digested with RNase R (Epicentre, Madison, WI, USA) at 37 °C for 30 min to remove linear RNAs.

Next-generation sequencing (NGS) and circRNA identification

The procedures for NGS analysis were performed as in our previous study with some modifications [23]. After RNA extraction, the obtained RNA depleted the ribosomal RNA using the RiboMinus kit (KAPA, USA) according to the protocol. The ribosome RNA-depleted RNA was further digested with RNase R (Epicentre) at 37 °C for 30 min to remove linear RNAs. Both the ionomycin group and the control group were repeated three times. The obtained RNA was quantified at OD260nm using the ND-1000 spectrophotometer (Nanodrop Technology, USA). The quality of purified RNA was evaluated using the Bioanalyzer 2100 (Agilent Technology, USA) with the RNA 6000 LabChip Kit (Agilent Technologies, USA). The SureSelect XT HS2 mRNA Library Preparation kit (Agilent, USA) was used for construction. AMPure XP beads (Beckman Coulter, USA) were used for size selection. Sequencing was performed using Illumina's sequencing-by-synthesis (SBS) technology (Illumina, USA), and sequencing results (FASTQ reads) were generated using Welgene Biotech's pipeline based on Illumina's base-calling program bcl2fastq v2.20. The NGS results have been uploaded to the Gene Expression Omnibus (GEO) of the National Center for Biotechnology Information and can be accessed at [GEO: GSE278650]. Candidate circRNAs were identified by CIRIquant, a novel algorithm for accurate circRNA quantification and differential expression analysis [24]. The NGS deep sequencing and bioinformatic analysis were conducted by Welgene Biotech. Co., Ltd. (Taipei, Taiwan). The NGS result was identified based on the circAtlas database (http://circatlas.biols.ac.cn) [25].

Preparation of cell lysates and nuclear extract for NFAT analysis

Jurkat cells after stimulated with ionomycin or ionomycin with PMAs for one hour were lysed using 1% NP-40 (Sigma-Aldrich) with the addition of a phosphatase inhibitor cocktail (Thermo Fisher Scientific, Waltham, USA) and a protease inhibitor cocktail (Sigma-Aldrich). Nuclear extracts were obtained using the Nuclear Extract Kit (Active Motif, Carlsbad, CA, USA) according to the manufacturer's protocol. Protein concentration was measured using the Bradford method.

Transfection study

Jurkat cells were transfected with either the plasmid pcDNA3.1(+) CircRNA Mini Vector encoding circ-CAMTA1 or the plasmid pcDNA3.1 linear form circ-CAMTA1 (both from Addgene plasmid repository, Watertown, Massachusetts, USA) by electroporation, as our previous study with some modification [10]. The schematic diagram of construct plasmid for circ-CAMTA1 and linear form of circ-CAMTA1 were showed in supplementary Figs. 1 and 2. Control groups were transfected with the respective empty plasmid. The transfected cells were further cultured in RPMI-1640 medium with 10% fetal calf serum at 37 °C with 5% CO_2 for 24–48 h in the presence or absence of PMA (20 ng/mL) and ionomycin (500 ng/mL). After centrifugation, cells were collected for the analysis of mRNA or protein expression.

RNA pull-down assay

RNA pull-down assays were performed as previously described [10]. Biotin-labeled circ-CAMTA1 was prepared in vitro using the plasmid pcDNA3.1(+) CircRNA Mini Vector encoding circ-CAMTA1 by T7 RNA polymerase (Ambion Inc., Austin, TX, USA) in the presence of a biotin RNA labeling kit (Biotin RNA Labeling Mix Roche, Basel, Switzerland). Control biotin-labeled RNAs were transcribed from the empty vector of pcDNA3.1(+) CircRNA Mini Vector. The products were purified with the RNeasy Mini Kit (Qiagen Hilden, Düsseldorf Germany). Custom circ-CAMTA1 containing junctional sequences (bio-CAMTA1JS) (5′-bio-AAACTGGAACAC TAATGAGGCACAAGGAAGGACAG-3′) and its antisense oligonucleotides (ASO) (5′-bio-AAACTGTCCTT CCTTGTGCCTCATTAGTGTTCCAGT-3′) were synthesized by Life Technologies company (Waltham, Massachusetts, USA).

For the pull-down of intracellular proteins, biotin-labeled RNA was mixed with 1.5 mg of Jurkat cell extract

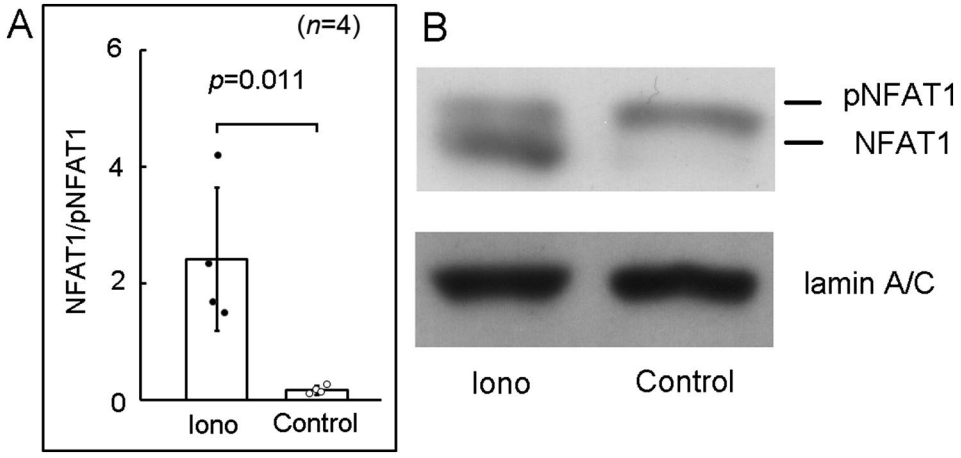

Fig. 1 Dephosphorylation of NFAT1 in Jurkat cells after coculture with ionomycin (1 μg/ml) for 1 h. (**A**) The addition of ionomycin significantly increased the ratio of dephosphorylated NFAT1 compared with the controls in nuclear extract of Jurkat cells. (**B**) A representative example

at 4 °C for 2 h, followed by the addition of washed streptavidin-coupled Dynabeads (Thermo Fisher Scientific). The precipitates were washed four times with IP buffer and collected by centrifugation (760 × g) at 4 °C for 2 min. The eluted proteins were separated by SDS-PAGE, followed by silver staining (Thermo Fisher Scientific) or Coomassie Blue staining. Differentially expressed protein bands identified by silver staining were cut from the gel after Coomassie Blue staining and sent for protein identification. The samples underwent in-gel digestion with trypsin and were analyzed using NanoLC-MS/MS with an integrated nano LC-MS/MS QSTAR XL System (Applied Biosystems, Waltham, Massachusetts, USA). The LC-MS/MS analysis was performed by Mission Biotech (Taipei, Taiwan).

To characterize the preferred binding, bio-CAMTA1JS (0.5 μg) with or without ASO (Mission Biotech, Taipei, Taiwan) was dissolved in 1 mL of IP buffer with 1.5 mg of cell extract at 4 °C for 2 h. Streptavidin-coupled Dynabeads (60 μL) were added, and the mixture was further incubated at 4 °C for 1 h. Beads were washed four times with IP buffer and analyzed by Western blotting.

Western blot analysis

Western blot analysis was performed using Jurkat cells as previously described [26]. Antibodies used for Western blot analysis included rabbit monoclonal antibodies against NFAT1 (#4389, Cell Signaling Technology, Danvers, MA, USA), rabbit monoclonal antibodies against PKR (#12297, Cell Signaling Technology, Danvers, MA, USA), and rabbit polyclonal antibodies against pyruvate carboxylase (PC) (GTX132002, GeneTex, Irvine, CA, USA). Rabbit monoclonal antibodies against lamin A/C (tcba178, Taiclone, Taipei, Taiwan) and anti-β-actin antibodies (sc-47778, Santa Cruz Biotechnology, Dallas, Texas, USA) were used as internal control.

RNA immunoprecipitation (RIP)

RIP assays were performed using the Magna RIP® RNA-Binding Protein Immunoprecipitation Kit (Sigma-Aldrich) according to the manufacturer's protocol. Briefly, Jurkat cells were collected and lysed using a lysis buffer provided by the kit. Anti-PC antibodies (GTX132002, GeneTex, Irvine, CA, USA) or Rabbit Control IgG provided by the kit were used to prepare the magnetic bead-conjugated antibodies for immunoprecipitation according to the kit instructions. RNA-binding protein-RNA complexes were immunoprecipitated with magnetic bead-conjugated antibodies at 4 °C overnight with agitation. The complexes were precipitated using protein G Dynabeads (40 μL per IP reaction). After washing the beads with ice-cold RIP Wash Buffer from the Magna RIP kit, the RNA-binding proteins were digested with proteinase K at 55 °C for 30 min with shaking. RNA was then isolated using the RNA Clean & Concentrator-5 kits (Zymo Research, Irvine, CA, USA) and analyzed using RT-PCR.

Enzyme-linked immunosorbent assay (ELISA)

Transfected Jurkat cells after stimulation with PMA (20 ng/mL) and ionomycin (500 ng/mL) for 48 h, the cell-free supernatants were collected by centrifugation at 300 x g for 10 min and were stored at -80℃ until analysis. Cytokine concentrations in the culture supernatants were determined using respective ELISA kits (BD Biosciences, Franklin Lakes, USA) according to the manufacturer's protocol.

Preparation of pyruvate carboxylase

Pyruvate carboxylase was prepared according to previously described methods with modifications [27]. The vector, pCDNA-3.1-PC, encoding His-tag pyruvate carboxylase, was ordered from Mission Biotech (Taipei,

Taiwan). 293T cells were transfected with pCDNA-3.1-PC by electroporation and maintained in Dulbecco's Modified Eagle's Medium (DMEM) with 10% fetal bovine serum, 2 mM L-glutamine, neomycin (500 μg/mL) and 5% CO_2 at 37℃. After antibiotic selection, surviving cells expressing His-tag pyruvate carboxylase were cultured in DMEM containing 10% fetal bovine serum, 2 mM L-glutamine, neomycin (500 μg/mL) and 5% CO_2 at 37℃ for 2 days. 293T cells were harvested by centrifugation. Mitochondria were isolated as described [27]. In brief, cells were suspended and homogenized at 4 °C for 2–3 min. Then the intact cells and cell nuclei were removed by centrifugation at 600 g at 4 °C for 20 min. The supernatant containing mitochondria was further centrifuged at 15,000 g at 4 °C for 30 min. Mitochondrial proteins were extracted using a buffer containing 20 mM Tris-HCl, pH 7.9, 0.5% NP40, 4 mM benzamidine, 0.02% sodium azide, 5 mM imidazole, and 0.5 M NaCl. The extracted proteins were purified by Ni^{2+}-Sepharose chromatography, followed by gel filtration using Sephacryl-200. Fractions containing His-tag pyruvate carboxylase were pooled and subjected to affinity chromatography using avidin-conjugated agarose as described [27]. The fractions containing His-tag pyruvate carboxylase were pooled, concentrated to 0.5 mL, and stored at 4℃ before use.

Measurement of pyruvate carboxylase activity and glucose levels

Jurkat cells were transfected with plasmid encoding circ-CAMTA1 or empty plasmid according to method mentioned previously [10]. After 48 h, pyruvate carboxylase enzymatic activity in these cells was measured using a commercial spectrophotometric pyruvate carboxylase activity kit (CAK1262, Cohesion, UK). For direct interaction of RNA and pyruvate carboxylase, 10 μL of the purified pyruvate carboxylase (protein concentration of 0.031 μg/μL) was mixed with CAMTA1JS (0.1 μg) or CAMTA1JS (0.1 μg)+ASO (0.1 μg) for 30 min, and then the mixture was analyzed for pyruvate carboxylase activity. After transfection with the plasmid encoding circ-CAMTA1 or its linear form for 24 h, Jurkat cells were cultured for 16 h, and the extracellular glucose levels in the culture supernatant were measured. Control groups were transfected with the respective empty plasmid. Glucose concertation was measured using a glucose assay kit (Abcam, Cambridge, UK) according to the manufacturer's instructions.

Table 1 Demographic and clinical data of patients with systemic lupus erythematosus and healthy controls

	SLE patients (*n* = 42)	Healthy controls (*n* = 23)	*P*
Age, mean years ± SD	41.4 ± 11.0	41.7 ± 4.0	0.685
Sex, female/male	35/7	20/3	> 0.999
SLEDAI-2 K score	4.6 ± 3.7		
Anti-double stranded DNA (IU/mL)	24.1 ± 38.8		
Complement C3 (mg/dL)	99.0 ± 23.5		
Lupus nephritis	40.5% (17/42)		
Medication			
Corticosteroids	90.5% (38/42)		
Steroid dosage equivalence to prednisolone (mg/day)	5.6 ± 4.1		
Hydroxychloroquine	90.5% (38/42)		
Mycophenolic acid	33.3% (14/42)		
Azathioprine	21.4% (9/42)		
Cyclosporine	7.1% (3/42)		
Rituximab	9.5% (4/42)		

NA, not applicable; SLE, systemic lupus erythematosus; SLEDAI-2 K, Systemic Lupus Erythematosus Disease Activity Index 2000 (SLEDAI-2K)

Measurement of RNA expression levels by RT-PCR

Total RNA was obtained using the Quick-RNA Mini-Prep kit (Zymo Research), and RNA concentration was quantified using a spectrophotometer (NanoDrop 1000, Thermo Fisher Scientifi). RNA expression levels were quantified by real-time RT-PCR using a one-step RT-PCR kit (TaKaRa, Shiga, Japan) with an ABI Prism 7500 Fast Real-Time PCR system (Applied Biosystems, Waltham, MA, USA) as previously described [22]. Glyceraldehyde-3-phosphate dehydrogenase (GAPDH) was used as a control for circRNAs, and 18 S ribosomal RNA was used for mRNA. To specifically amplify the circRNAs, the primers were designed to span the circRNA back-splice junction sequence. This ensures they specifically amplify circRNAs, and not the linear forms with the same sequence. The primers used are listed in the Supplementary Table 1.

Detection of Jurkat cell activation by flow cytometry

Jurkat cells after transfection with the plasmid encoding circ-CAMTA1 or empty plasmid were cocultured with ionomycin and PMA for 24 h. The percentage of activate Jurkat cells was determinate by staining with mouse monoclonal anti-human CD25 conjugated with FITC (565096, Becton Dickinson, Franklin Lakes, NJ, USA) and FITC Mouse IgG1, Isotype Control (555748, Becton Dickinson, Franklin Lakes, NJ, USA) was used as control. The result was analyzed by flow cytometry (FACSMelody, Becton Dickinson, Franklin Lakes, NJ, USA).

Cell viability and proliferation using mitochondrial dehydrogenase cleavage assay

Jurkat cells after transfection with the plasmid encoding circ-CAMTA1 or empty plasmid were cocultured with ionomycin and PMA for 24 h. Then 10 μL WST-1 (Roche Diagnostics, Basel, Switzerland) was added and incubated for 4 h. The intensity of color formation was

detected using SpectraMax iD5 Multi-Mode Microplate Reader (Molecular Devices, San Jose, CA) at 440 nm.

Statistical analysis

Statistical significance was assessed using the Student's t-test or Mann-Whitney U-test, as appropriate. Simple and multiple linear regression analyses were performed to investigate the association between specific circRNA expression levels and clinical parameters of SLE. Statistical analyses were performed using Stata software (StataCorp, College Station, TX, USA).

Results

Dephosphorylation of NFAT1 by ionomycin

The dephosphorylation form of NFAT1 increased in nuclear protein extracts following coculture with ionomycin for 1 h (Fig. 1A and B).

Identification and validation of Ca2+ influx-regulated circRNAs

Using next-generation sequencing (NGS) analysis, we found that the expression levels of 67 circRNAs were upregulated, and 57 circRNAs were downregulated following Ca^{2+} influx (Fig. 2A). Detailed circular RNA information is provided in Supplementary Table 2. After excluding low expression circRNAs, we selected 12 upregulated circRNAs and two downregulated circRNAs for further validation. After validation, we confirmed that the expression levels of circ-ERCC4, circ-NFATC2, circ-MYH10, circ-CAMTA1, circ-ASH1L, circ-SOCS7, and circ-ASAP1 consistently increased in Jurkat cells after Ca^{2+} influx (Fig. 2B).

Expression profile of Ca^{2+}influx-regulated circRNAs in T cells from patients with SLE and healthy controls and its association with SLE disease activity

We investigated the expression levels of the Ca^{2+} influx-regulated circRNAs in T cells from 42 patients with SLE and 23 healthy controls. The demographic data was provided in Table 1, showing no statistically significant differences in age or female-to-male ratio between the two groups. Among the Ca^{2+} influx-regulated circRNAs, circ-CAMTA1, circ-ASH1L, and circ-ASAP1 expression levels were significantly lower in T cells from patients with SLE compared to healthy controls (Fig. 3A). We further categorized disease activity into lower (SLEDAI-2K<3), and higher (SLEDAI-2K≥ 3) SLE disease activity based on a previous study [28]. As shown in Fig. 3B, the expression levels of circ-CAMTA1, circ-ASH1L, and circ-ASAP1 were significantly lower in T cells from SLE patients with higher disease activity compared to those with lower disease activity.

As shown in Table 2, only SLE disease activity, not age, sex, serum anti-double stranded DNA levels, serum complement C3 levels, history of lupus nephritis, steroid dosage, or the use of potent immunosuppressants, was associated with the expression levels of circ-CAMTA1, circ-ASH1L, and circ-ASAP1. After adjusting for age and sex, T cells from SLE patients with higher disease activity remained to show significantly lower expression levels of circ-CAMTA1 (0.30-fold; $P<0.001$), circ-ASH1L (0.35-fold; $P=0.009$), and circ-ASAP1 (0.27-fold; $P<0.001$) compared to those from patients with lower disease activity. A scatter plot for the expression levels of circ-CAMTA1 and SLEDAI-2K scores was showed in supplementary Fig. 3.

Expression levels of Ca2+ influx-regulated circRNA in jurkat cells after stimulation

The expression levels of circ-CAMTA, circ-ASH1L, and circ-ASAP1 were significantly increased in Jurkat cells following coculture with PMA and ionomycin (Fig. 4A and B, and 4C), paralleling the effect of ionomycin. After coculture with IFN-α for 72 h, the expression level of circ-CAMTA (Fig. 4D) significantly decreased, whereas circ-ASH1L (Fig. 4E) and circ-ASAP1 (Fig. 4F) did not.

Circ-CAMTA1 interacted with pyruvate carboxylase protein

Following RNA immunoprecipitation (RNA-IP), four reactive protein bands with molecular weights of 130, 110, 50, and 45 kDa were excised and subjected to proteomic analysis (Fig. 5A). The identified proteins included pyruvate carboxylase in the 130-kDa band, heat shock protein HSP 90 in the 110-kDa band, elongation factor 1-alpha in the 50-kDa band, and actin in 45 kDa band. We chose pyruvate carboxylase for further investigation. RNA pull-down followed by Western blotting analysis confirmed that circ-CAMTA1 bound to pyruvate carboxylase protein (Fig. 5B). Using RIP with an anti-pyruvate carboxylase antibody, we found that the pyruvate carboxylase could interact with circ-CAMTA1 (Fig. 5C). Since the pyruvate carboxylase is a biotin-containing enzyme [29], we performed RIP with custom circ-CAMTA1 containing junctional sequences (bio-CAMTA1JS) with/without its antisense oligonucleotides (ASO) or streptavidin alone. We found that bio-CAMTA1JS, but not streptavidin, could interact with pyruvate carboxylase (Fig. 5D), and the addition of ASO could block this interaction. Transfection with a plasmid encoding circ-CAMTA1 suppressed pyruvate carboxylase activity compared to controls (Fig. 5E). Cloning and purification of pyruvate carboxylase for in vitro analysis showed that the addition of ASO could reverse the suppressive effect of pyruvate carboxylase activity mediated by CAMTA1JS (Fig. 5F).

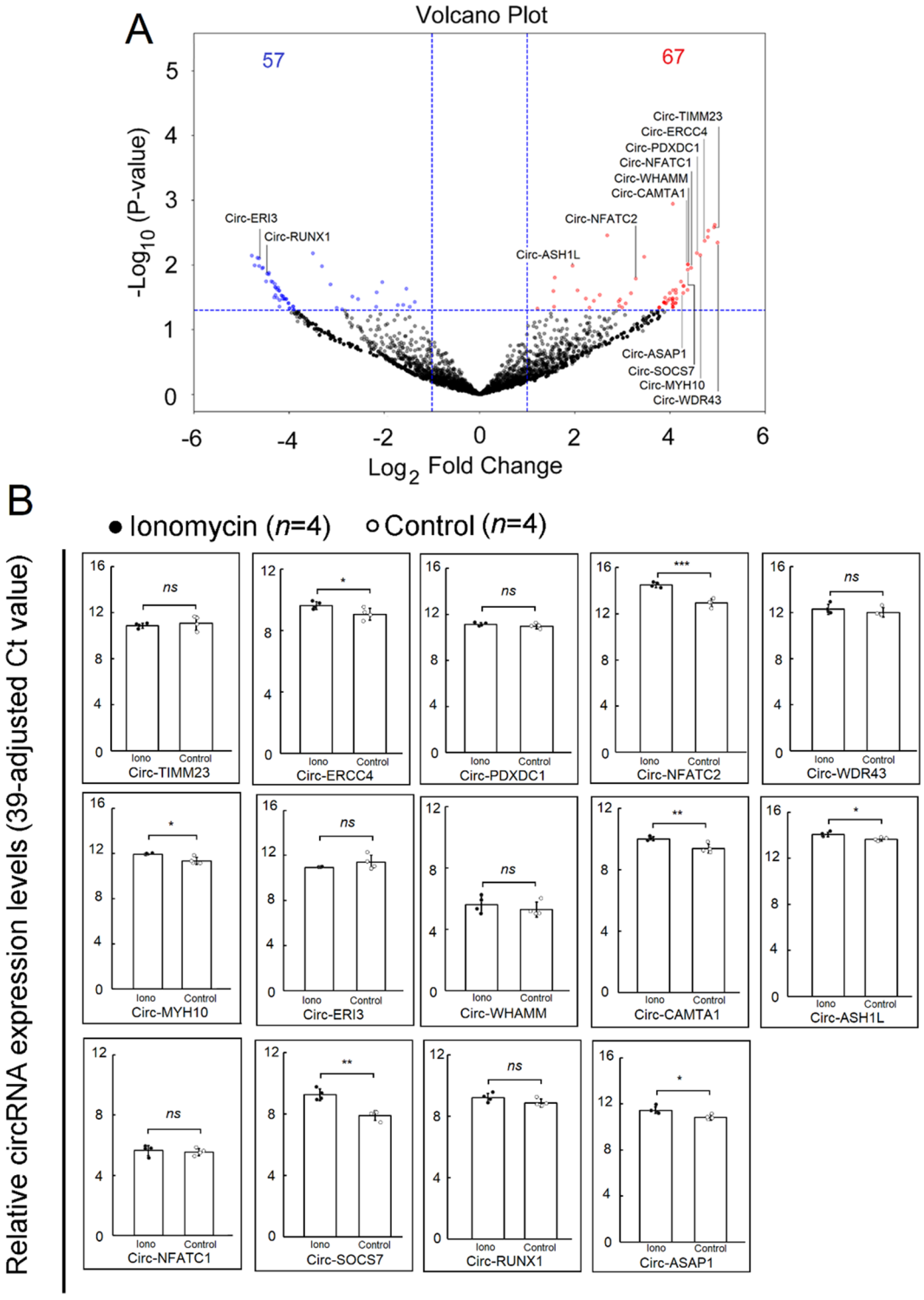

Fig. 2 Differential expression of circRNA in Jurkat cells after coculture with ionomycin (1 μg/mL) for 1 h. (**A**) The expression profiles of circRNA in Jurkat cells after coculture with ionomycin (1 μg/mL) for 1 h were evaluated using next-generation sequencing. Each scatter point in the figure represents the mean read count of circRNA in three replicates of the treatment. (**B**) Validation of potential candidates of Ca^{2+} influx-regulated circRNAs in Jurkat cells. The relative expression level of circRNA was defined as (39 - Ct) after adjusted with the internal control (GAPDH; Glyceraldehyde-3-Phosphate Dehydrogenase). Data was presented as mean ± SD. (ns, not significant; *$P < 0.05$; **$P < 0.01$; ***$P < 0.001$)

Table 2 Regression analyses assessing the correlations between the expression levels of circRNA transcripts with demographic data of patients with systemic lupus erythematosus

Variable	circ-CAMTA1	circ-ASH1L	circ-ASAP1
Sex (male/female)	1.40 (0.62–3.16)	1.45 (0.50–4.24)	1.80 (0.68–4.78)
Age (per 10 years)	1.00 (0.75–1.32)	1.03 (0.71–1.49)	1.03 (0.73–1.51)
Higher SLE disease activity disease activity index score[b]	0.30 (0.18–0.49)**	0.34 (0.16–0.74)*	0.27 (0.14–0.51)**
Anti-double stranded DNA (per 10 IU/mL)	0.95 (0.88–1.02)	0.97 (0.87–1.07)	0.94 (0.85–1.03)
Complement C3 (per 10 mg/dL)	0.98 (0.86–1.11)	0.97 (0.82–1.15)	1.01 (0.86–1.18)
Lupus nephritis (yes/no)	1.00 (0.54–1.86)	0.76 (0.34–1.70)	1.07 (0.50–2.27)
Steroid dosage equivalence to prednisolone (mg/day)	0.98 (0.91–1.06)	0.96 (0.87–1.05)	0.47 (0.14–1.61)
Potent immunosuppressants[a] (yes/no)	1.24 (0.67–2.30)	1.16 (0.51–2.62)	1.19 (0.56–2.51)

Data was presented as fold change with 95% confidence interval. *$P<0.05$; **$P<0.001$)

The disease activity was further categorized as: lower disease activity: SLEDAI-2 K < 3, higher disease activity SLEDAI-2K ≥ 3

[a]Patients with systemic lupus erythematosus received azathioprine, mycophenolic acid, cyclosporine, or rituximab in addition to steroid and hydroxychloroquine

[b]After adjusting for age and sex, the T cells form SLE patients with higher disease activity remained to have lower expression levels of circ-CAMTA1 ($P<0.001$), circ-ASH1L ($P=0.009$), and circ-ASAP1 ($P<0.001$) compared with those from SLE patients with lower disease activity

Increased expression of circ-CAMTA1, but not its linear form, significantly decreased extracellular glucose levels

Pyruvate carboxylase is the first step and key regulator of gluconeogenesis [30]. We hypothesized that the inhibitory effect of circ-CAMTA1 on pyruvate carboxylase could impair gluconeogenesis. Enhanced expression of linear form circ-CAMTA1 (linear-CAMTA1) slightly decreased extracellular glucose levels compared to controls (Fig. 5G). Enhanced expression of circ-CAMTA1 significantly decreased extracellular glucose levels compared to controls or its linear form. After stimulation with PMA/ionomycin, expression of linear-CAMTA1 slightly increased the extracellular glucose levels compared to controls, while enhanced expression of circ-CAMTA1 significantly decreased extracellular glucose levels compared to controls or its linear form (Fig. 5H).

Increased expression circ-CAMTA1, but not its linear form, enhanced IL-2 secretion

Following transfection, the expression of circ-CAMTA1 was significantly increased (Fig. 6A). Enhanced expression of circ-CAMTA1 increased the IL-2 secretion, but not the *IL-2* mRNA expression, in Jurkat cells after stimulation (Fig. 6B and C). Increased expression of linear form circ-CAMTA1 (linear-CAMTA1) was also confirmed after transfection (Fig. 6D). Increased expression of linear form hsa-CAMTA1_0020 did not affect the production of IL-2 or *IL-2* mRNA expression (Fig. 6E and F). Liu et al. demonstrated that some circRNAs could form 16–26 bp duplexes and inhibit the activation of double-stranded RNA (dsRNA)-activated protein kinase (PKR) [31]. Activation of PKR contributes to the production of proinflammatory cytokines [32]. We showed that the transfection of circ-CAMTA1 did not result in the activation of PKR (Fig. 6G). Furthermore, increased expression of circ-CAMTA1, or its linear form, did not affect the dephosphorylated NFAT1protein levels (Fig. 6H and I).

Overexpression of circ-CAMTA1 for the activation or proliferation of jurkat cells and miRNA-181c-5p expression

We found that higher percentage of CD25 positive cells in Jurakt cells transfected with circ-CAMTA1 compared with those transfected with the empty plasmidafter stimulated with PMA and ionomycin (Fig. 7A). Also, overexpression of circ-CAMTA1 could enhance the proliferation of Jurkat cells after stimulation (Fig. 7B). Overexpression of circ-CAMTA1, but not its linear form, decreased miR-181c-5p expression in Jurkat cells after stimulation (Fig. 7C and D).

Discussion

Calcium signaling affects the proliferation, differentiation, and cytokine secretion in T cells [33]. Several studies have shown that circRNAs could affect Ca^{2+} influx [34, 35]. In this study, we originally found that Ca^{2+} influx could upregulate the expression of circRNAs. Abnormal Ca^{2+} influx and its signaling pathway have been documented in SLE T cell. Therefore it is not surprising that the expression levels of several Ca^{2+} influx-regulated circRNAs, including circ-CAMTA1, circ-ASH1L, and circ-ASAP1 were significantly lower in T cells from patients with SLE. We also demonstrated that IFN-α, a key cytokine for the pathogenesis of SLE, decreased the expression levels of circ-CAMTA1. Therefore, we speculated that IFN-α could contributed to the abnormal Ca^{2+} signaling pathway in SLE T cells. Since increased circ-CAMTA1 expression could enhance IL-2 expression in Jurkat cells after stimulation. The decrease expression of circ-CAMTA1 in SLE T cells might contributed to the decreased IL-2 secretion in SLE T cells. We also found that the expression levels of these circRNAs were significantly lower in T cells from SLE patients, especially those with moderate and high disease activity. This correlation between circRNA levels and disease activity in SLE patients aligns with other studies showing aberrant circRNA expression in plasma or PBMCs, suggesting their potential utility in diagnosing and monitoring disease activity in patients with SLE [14]. However, our

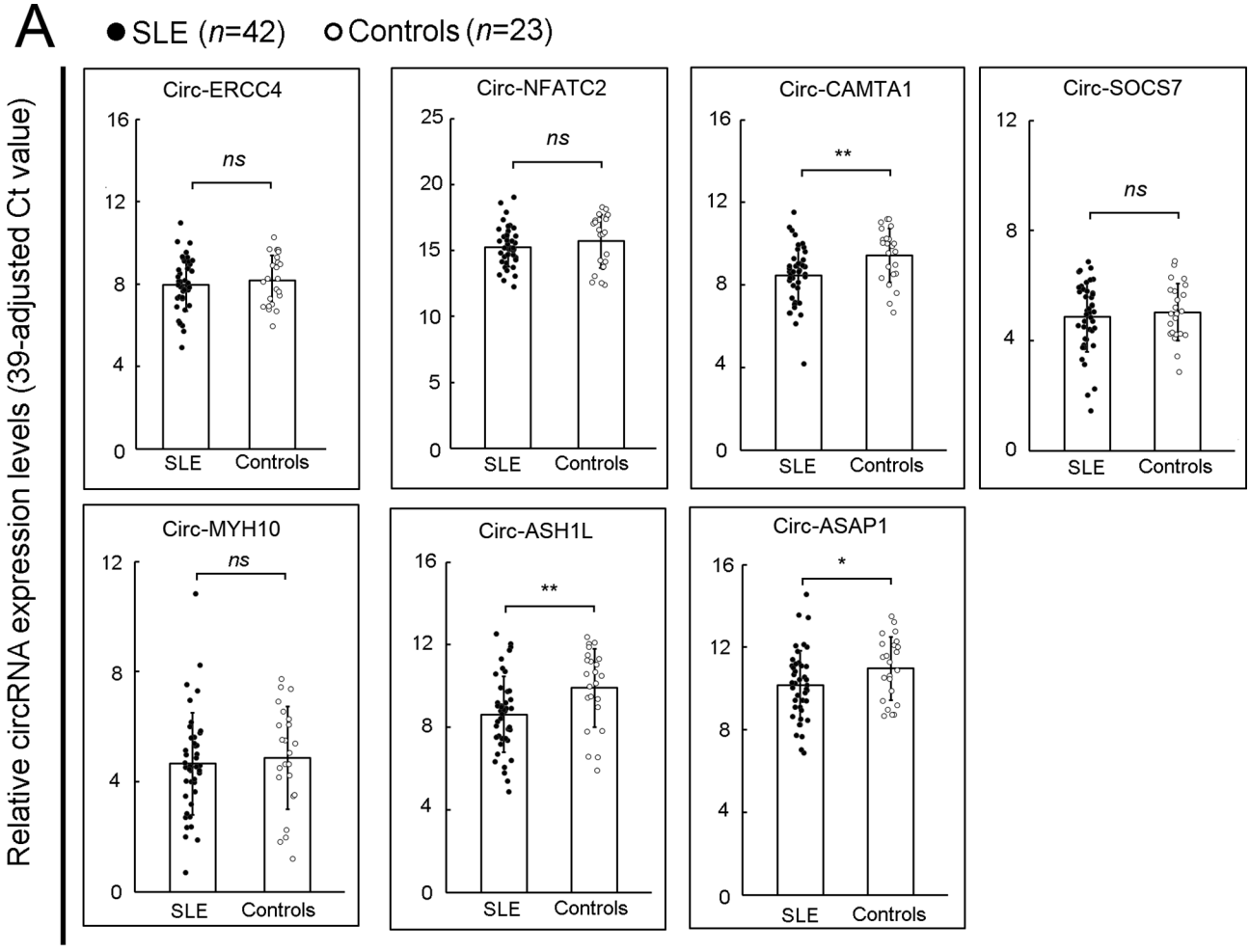

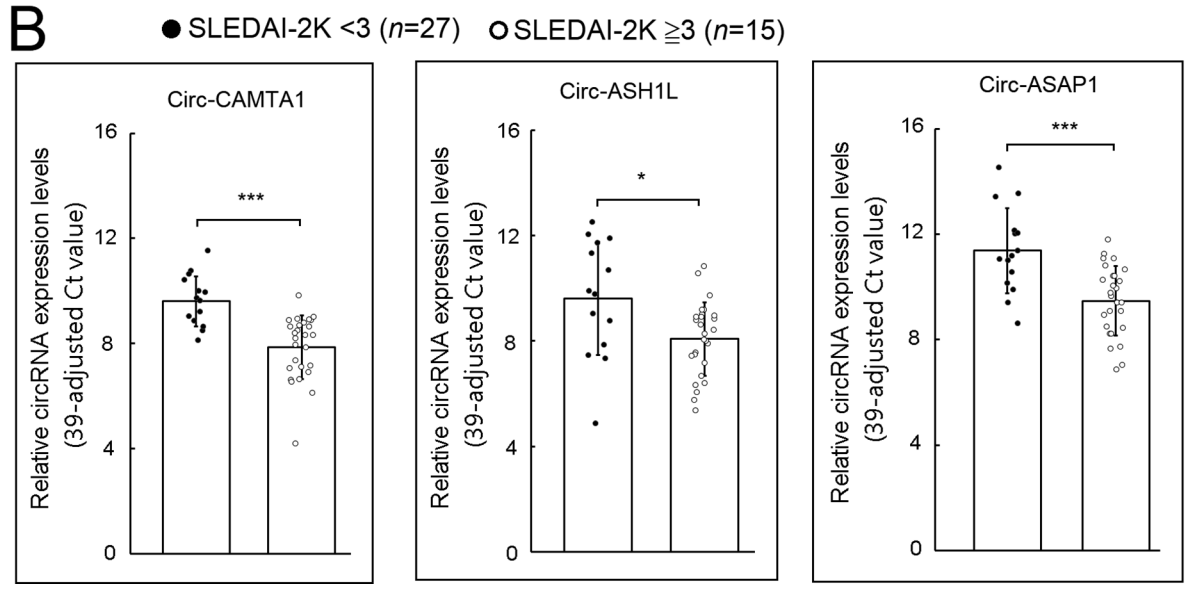

Fig. 3 (See legend on next page.)

(See figure on previous page.)

Fig. 3 Differential expression of Ca^{2+} influx-regulated circRNA in T cells from patients with SLE and controls and its association with SLE disease activity (**A**) The expression of the seven Ca^{2+} influx-regulated circRNAs in T cells from patients with SLE and controls. The relative expression level of miRNA was defined as 39 - Ct, adjusted with the internal control. The expression levels of circ-CAMTA1, circ-ASH1L, and circ-ASAP1 were significantly lower in T cells from patients with SLE. After adjusting for age and sex, the SLE T cells still had lower expression levels of circ-CAMTA1 ($P=0.008$), circ-ASH1L ($P=0.008$), and circ-ASAP1 ($P=0.046$). (**B**) The expression levels of circ-CAMTA1, circ-ASH1L, and circ-ASAP1 in T cells from patients with SLE with different disease activity. The disease activity of SLE was measured by Systemic Lupus Erythematosus Disease Activity Index 2000 (SLEDAI-2K). The disease activity was further classified as: lower disease activity SLEDAI-2K < 3 and higher disease activity SLEDAI-2K ≥ 3. After adjusting for age and sex, T cells from SLE patients with higher disease activity still had lower expression levels of circ-CAMTA1 ($P<0.001$), circ-ASH1L ($P=0.009$), and circ-ASAP1 ($P<0.001$) compared to those from SLE patients with low disease activity. Data was presented as mean ± SD. (ns, not significant; *$P<0.05$; **$P<0.01$; ***$P<0.001$)

study only investigated the biological function of circ-CAMTA1, and the biological function of circ-ASH1L and circ-ASAP1 warrant further investigation.

Regarding the biological function of circRNAs, we found that increased expression circ-CAMTA1, but not its linear form, enhanced the secretion of IL-2. IL-2, a cytokine primarily produced by T cells, is crucial for T cell activation and proliferation. We demonstrated that overexpression of circ-CAMTA1 could enhanced Jurkat cells activation and proliferation upon stimulation. SLE T cells have reduced IL-2 secretion, contributing to the pathogenesis of SLE [36]. Recently, low-dose IL-2 injections have been considered a potential therapeutic strategy for patients with SLE [37]. The decreased circ-CAMTA1 expression could contribute to the reduced IL-2 secretion. However, overexpression of circ-CAMTA1 did not affected the mRNA expression of *IL-2*. After the mRNA transcription, several post-transcriptional mechanisms, such as mRNA localization, translation rate or translation inhibition by miRNAs, can influence the cytokines production [38, 39]. Notably, miR-181c-5p binds to the 3' UTR of the IL-2 mRNA and inhibits the IL-2 mRNA translation [39]. Our study confirmed that overexpression of circ-CAMTA1 suppressed

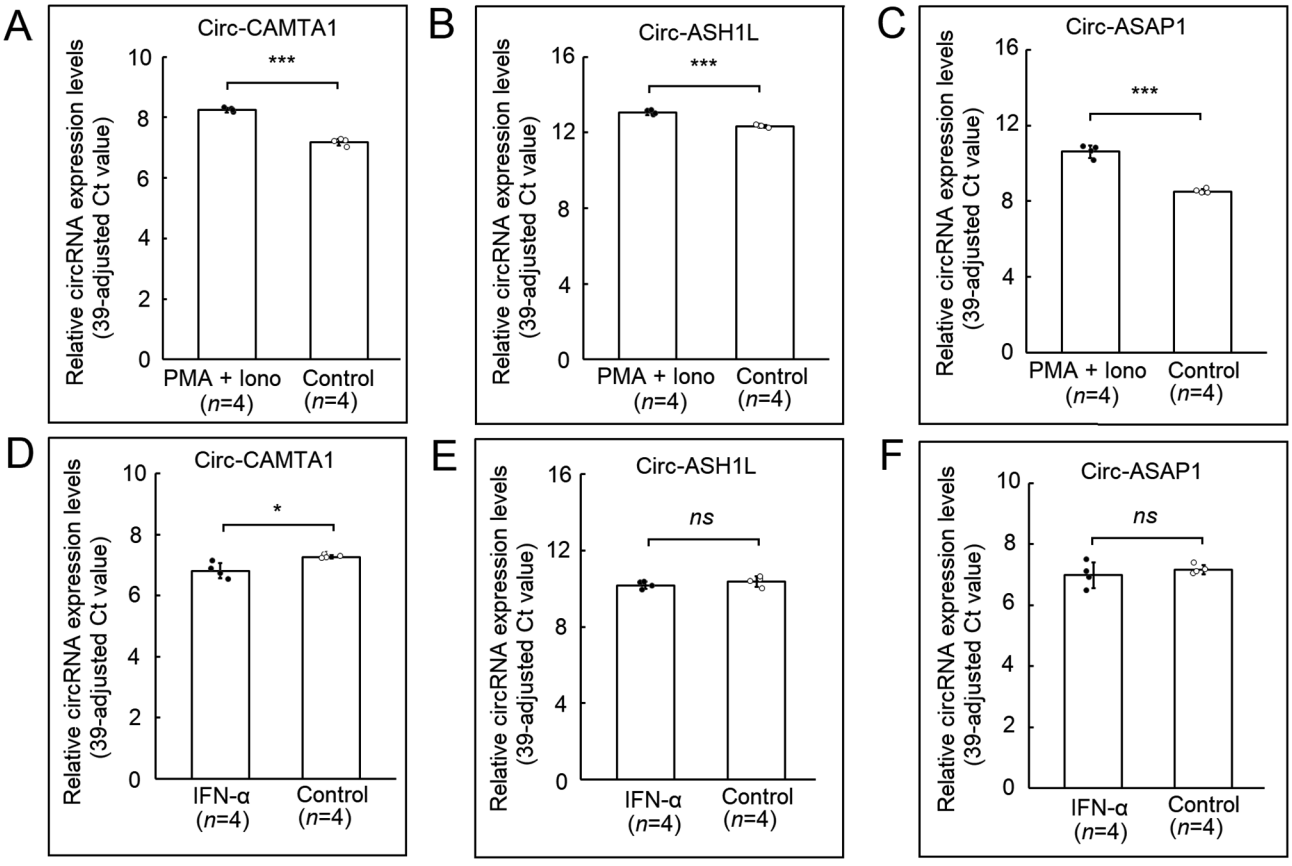

Fig. 4 The expression levels of circ-CAMTA1, circ-ASH1L, and circ-ASAP1 in Jurkat cells after stimulation. Jurkat cells were stimulated with PMA 20 ng/mL + Ionomycin (Iono) 500 ng/mL for 24 h. (**A**) The expression levels of circ-CAMTA. (**B**) The expression levels of circ-ASH1L. (**C**) The expression levels of circ-ASAP1. Jurkat cells were stimulated with 1000 IU/mL recombinant human interferon-alpha (IFN-α) for 72 h. (**D**) The expression levels of circ-CAMTA1. (**E**) The expression levels of circ-ASH1L. (**F**) The expression levels of circ-ASAP1. Data was presented as mean ± SD. (ns, not significant; *$P<0.05$; **$P<0.01$; ***$P<0.001$)

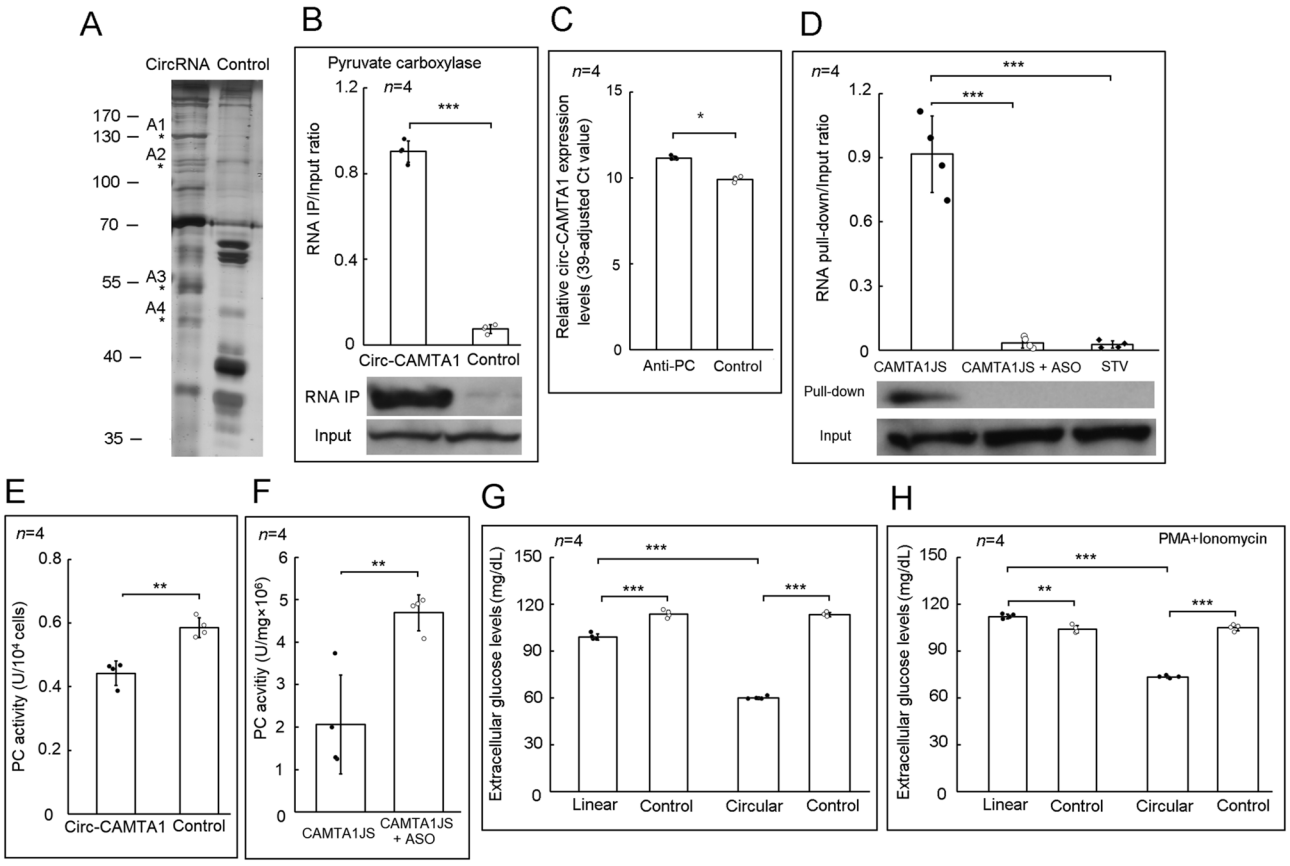

Fig. 5 Circ-CAMTA1 bound to pyruvate carboxylase protein and affected glucose metabolism. (**A**) Circ-CAMTA1, but not the control bound to four reactive protein bands with molecular weights of 130, 110, 50, and 45 kDa. Pyruvate carboxylase was identified in the 130-kDa band using LC-MS/MS analysis. (**B**) Circ-CAMTA1 bound to pyruvate carboxylase protein after RNA pull assay followed by Western blotting. (**C**) Using RNA-IP with anti-pyruvate carboxylase antibody, we found that pyruvate carboxylase bound to circ-CAMTA1 as well. (**D**) The result of RIP with a custom biotinylated fragment of circ-CAMTA1 containing junctional sequences (bio-CAMTA1JS) with/without its antisense oligonucleotides (ASO) or streptavidin only. (**E**) The transfection of circ-CAMTA1 or empty plasmid on the pyruvate carboxylase activity in Jurkat cells. (**F**) In vitro pyruvate carboxylase protein activity after addition CAMTA1JS with/without ASO. (**G**) After transfection of plasmid encoding circ-CAMTA1 or its linear form for 24 h, Jurkat cells were cultured for 16 h, and then the extracellular glucose levels of the culture supernatant were measured. The control groups were those transfected with the respective empty plasmid. (**H**) After transfection of plasmid encoding circ-CAMTA1 or its linear form for 24 h, Jurkat cells were further cultured with PMA (20 ng/mL) and ionomycin (500 ng/mL) for 16 h. The control groups were those transfected with the respective empty plasmid. Then, the glucose levels of the culture supernatant were measured. Data was presented as mean ± SD. (ns, not significant; *$P < 0.05$; **$P < 0.01$; ***$P < 0.001$)

miR-181c-5p expression in Jurkat cells after stimulation. In addition, circ-CAMTA1 bound to pyruvate carboxylase, and we confirmed that circ-CAMTA1 could suppress pyruvate carboxylase activity, which could be reversed by the addition of ASO. Cheng et al. also found that another lncRNA, RP11-241J12.3, could interact with pyruvate carboxylase [40]. We speculated that pyruvate carboxylase might have intrinsic RNA binding activity, which could affect its biological function.

Pyruvate carboxylase is a key regulatory enzyme in gluconeogenesis, converting pyruvate to oxaloacetate [41]. Gluconeogenesis involves the formation of glucose from non-carbohydrate substrates, with the liver being the principal organ for this process [42]. Besides pyruvate carboxylase, Jurkat cells express mitochondrial phosphoenolpyruvate carboxykinase (PEPCK-M), which can potentiate gluconeogenesis and tricarboxylic acid cycle flux [43]. Computational modeling by Baker et al. showed that genes related to gluconeogenesis, particularly PEPCK-M, might enhance the immunosuppressive effect of regulatory T cells [44]. Our findings showed that overexpression of circ-CAMTA1, but not its linear form, significantly decreased extracellular glucose levels. SLE T cells exhibited enhanced tricarboxylic acid cycle activity and oxidative phosphorylation [45], and inhibiting this metabolic pathway could suppress inflammatory responses in SLE animal models [46]. While few studies have investigated the possible effect of the gluconeogenesis pathway on T cell function. Shu et al. demonstrated that tumor-associated hypoxia suppressed pyruvate carboxylase expression in tumor-associated macrophages (TAMs), which in turn inhibited anti-tumor actions of

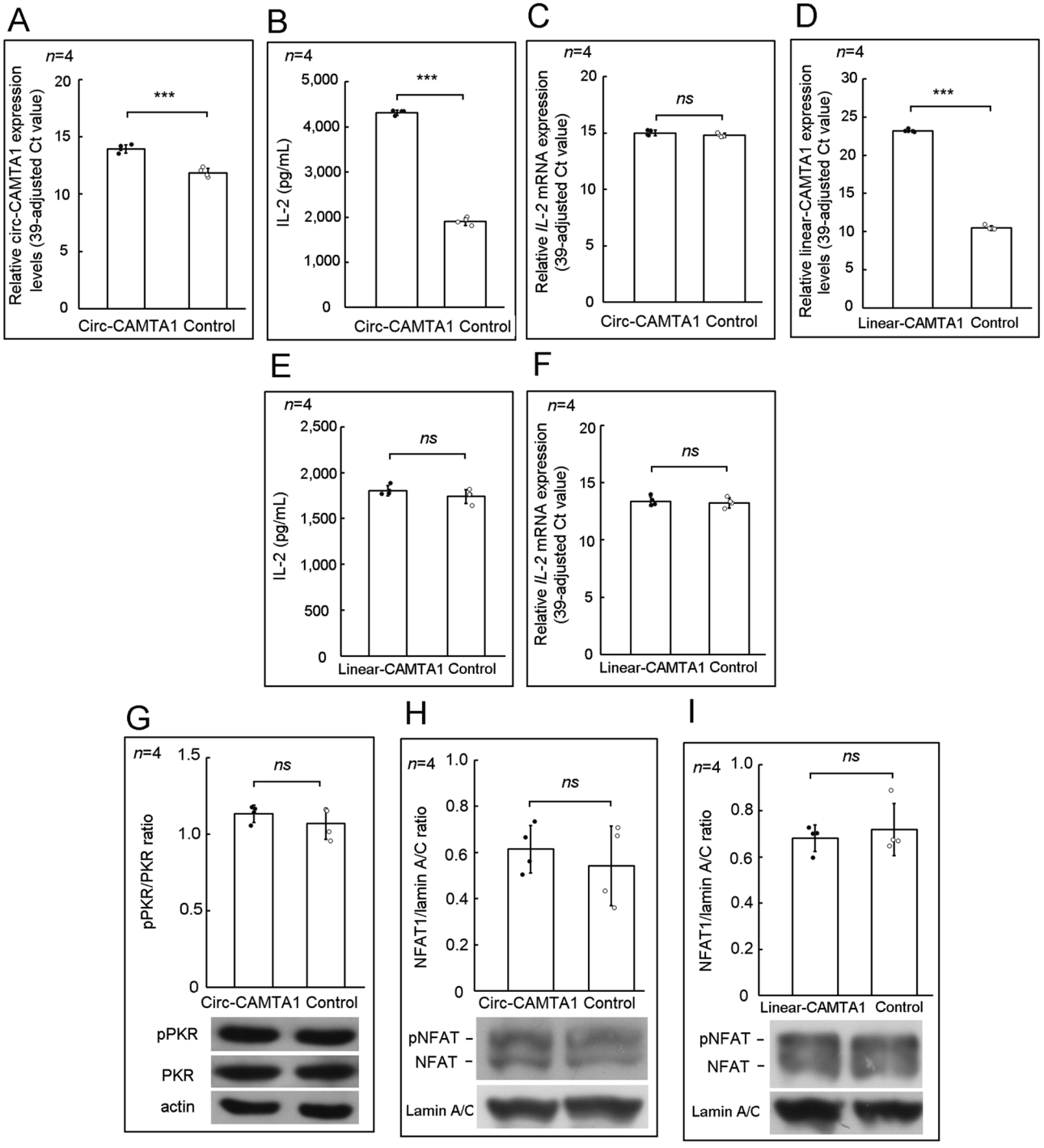

Fig. 6 Increased expression of circ-CAMTA1, but not its linear form (linear-CAMTA1), enhanced the secretion of IL-2. (**A**) The transfection of plasmid encoding circ-CAMTA1 increased the expression of circ-CAMTA1. (**B**) Overexpression of circ-CAMTA1 increased the IL-2 secretion after stimulation with PMA (20 ng/mL) and ionomycin (500 ng/mL) for 48 h. (**C**) Overexpression of circ-CAMTA1 did not increase the *IL-2* mRNA expression in Jurkat cells after stimulation. (**D**) The transfection of plasmid encoding linear-CAMTA1 increased the expression of linear-CAMTA1. (**E**) Increased expression of linear-CAMTA1 did not increase the IL-2 secretion in Jurkat cells after stimulation with PMA (20 ng/mL) and inomycin (500 ng/mL) for 48 h. (**F**) Increased expression of linear-CAMTA1 did not increase *IL-2* mRNA expression in Jurkat cells after stimulation. (**G**) The overexpression of circ-CAMTA1 did not affect the phosphorylation of double-stranded RNA (dsRNA)-activated protein kinase (PKR). (**H**) After stimulation with PMA and ionomycin for one hr. Increased expression of circ-CAMTA1 did not affect the protein expression of dephosphorylated NFAT1. (**I**) Increased expression of linear-CAMTA1 did not increase the protein expression of dephosphorylated NFAT1. Data was presented as mean ± SD. (ns, not significant; *$P < 0.05$; **$P < 0.01$; ***$P < 0.001$)

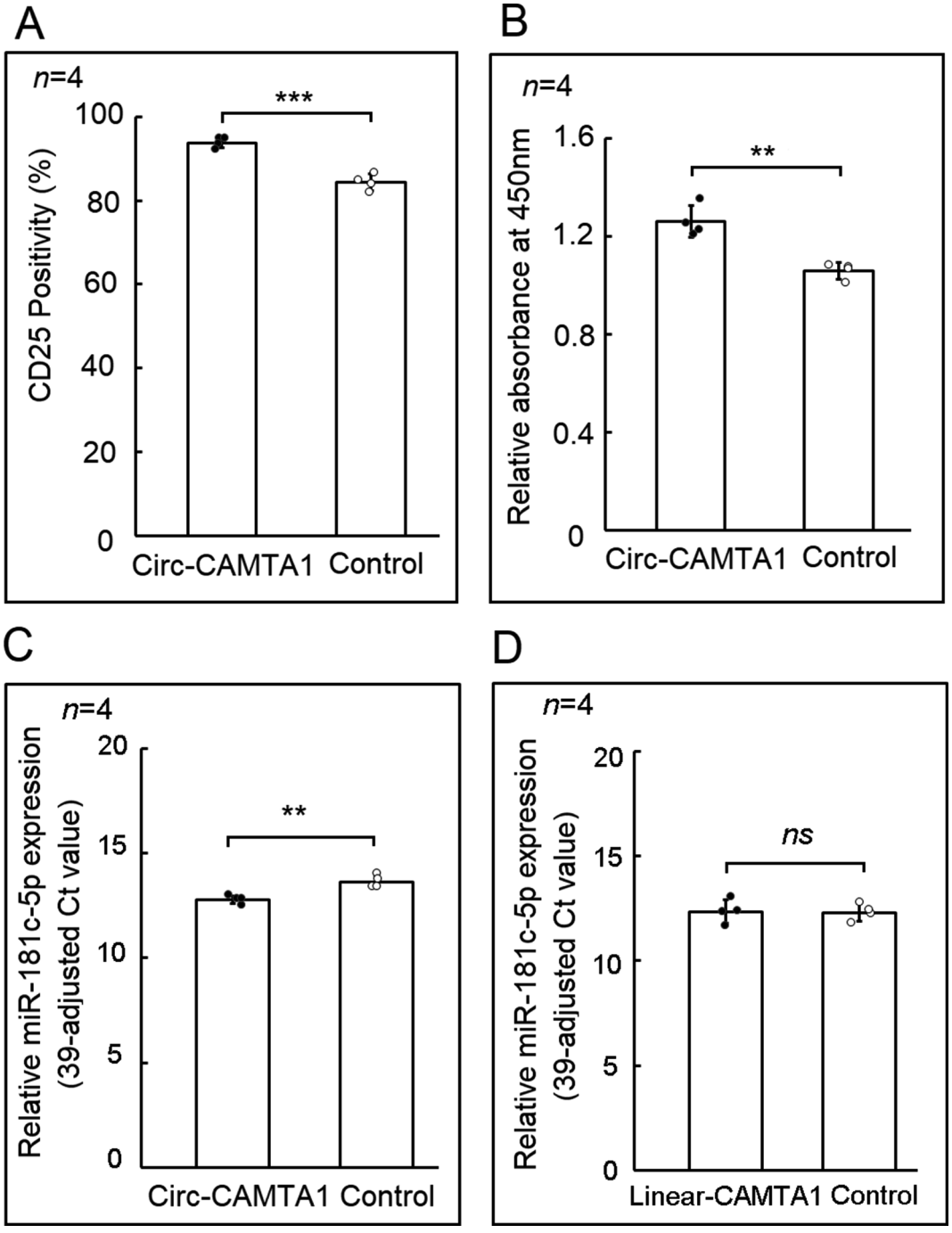

Fig. 7 Overexpression circ-CAMTA1 on the activation or proliferation of Jurkat cells and miR-181c-5p expression. (**A**) Jurkat cells after transfection with the plasmid encoding circ-CAMTA1 or empty plasmid were cocultured with ionomycin and PMA for 24 h. The percentage of activated Jurkat cells were defined as the positivity of CD25 analyzing using flowcytometry. (**B**) Jurkat cells after transfection with the plasmid encoding circ-CAMTA1 or empty plasmid were cocultured with ionomycin and PMA for 24 h. The proliferation and viability of cells was measured using mitochondrial dehydrogenase cleavage assay. (**C**) Jurkat cells after transfection with the plasmid encoding circ-CAMTA1 or empty plasmid were cocultured with ionomycin and PMA for 24 h. The expression of miR-181c was analyzed by real-time PCR (**D**) Jurkat cells after transfection with the plasmid encoding linear-CAMTA1 or empty plasmid were cocultured with ionomycin and PMA for 24 h. The expression of miR-181c-5p was analyzed by real-time PCR

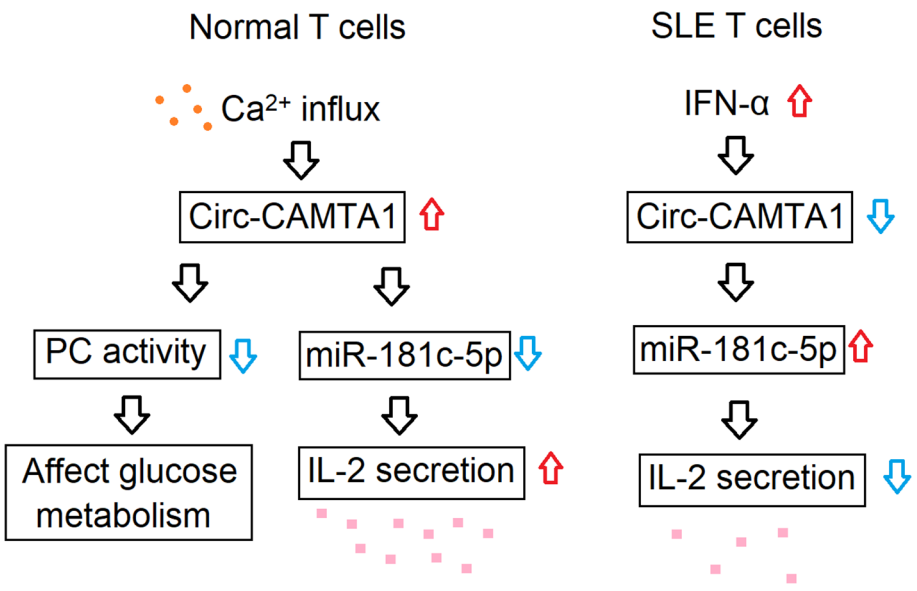

Fig. 8 Schematic model of the circ-CAMTA1 biological function in normal T cells and its potential pathogenic role in the SLE T cells

TAMs [47]. Furthermore, Liang et al. showed that Anemoside B4 (AB4), an abundant saponin isolated from *Pulsatilla chinensis* (Bunge), could ameliorate inflammation of 2, 4, 6-trinitrobenzene sulfonic (TNBS)-induced colitis in rats or dextran sulfate sodium (DSS)-induced colitis in mice through inhibiting pyruvate carboxylase activity [48]. The role of circ-CAMTA1 in gluconeogenesis and its potential implications for SLE treatment need further investigation.

We also observed that circ-CAMTA expression significantly decreased after coculture with IFN-α for 72 h. IFN-α plays a critical role in SLE immunopathogenesis [49], with elevated serum levels, detected by ultrasensitive single-molecule array digital immunoassay, could predict relapse in SLE patients in remission [50]. The most important part is that, blocking the IFN-α signaling pathway using a human monoclonal antibody against type I interferon receptor has been approved for treating SLE [51]. Liu et al. demonstrated that activation of the innate immune system by polyinosinic acid-polycytidylic acid or virus would trigger the activation of double-stranded RNA (dsRNA)-activated protein kinase (PKR), leading to global degradation of circRNAs [31]. However, we found that circ-ASH1L and circ-ASAP1 expression levels remained unchanged after IFN-α stimulation, and increased circ-CAMTA1 expression did not activate PKR. Further studies are needed to understand the mechanisms behind these observations. Our study indicated that Ca^{2+} influx could enhanced circ-CAMTA1 expression in normal T cells. Increased circ-CAMTA1 directly inhibited PC activity affecting glucose metabolism and reduced miR-181c-5p expression, which in turn increased IL-2 secretion. In SLE T cells, IFN-α inhibited circ-CAMTA1 expression, potentially resulting in decreased IL-2 secretion (Fig. 8).

The strengths of this study lies not only in identifying the differential expression of circRNAs in T cells from SLE patients compared to controls, but also in validating the binding of the protein PC to one of the identified circRNAs, circ-CAMTA1. Furthermore, we conduction functional analyses and demonstrated that circ-CAMTA1 can inhibit PC activity.

However, this study has some limitations. First only 42 SLE patients were enrolled, all from the outpatient clinic of a regional teaching hospital in southern Taiwan. A larger sample size, especially, including patients with more active disease, is needed to further validate the association between circ-CAMTA1 expression and SLE disease activity. Second, we did not investigate the potential interactions between circ-CAMTA1 and other proteins, such as HSP 90 or elongation factor 1-alpha. Further studies are required to explore these interaction.

Conclusion

In summary, our study found that Ca^{2+} influx regulated circRNAs expression. Among these circRNAs, circ-CAMTA1, circ-ASH1L, and circ-ASAP1 levels were significantly lower in T cells from SLE patients, particularly those with moderate and high disease activity. IFN-α suppressed circ-CAMTA1 expression, and transfection of circ-CAMTA1 decreased miR-181c-5p expression resulting increased IL-2 section and. Moreover, circ-CAMTA1 interacted with pyruvate carboxylase, affecting glucose metabolism. These findings suggest that circ-CAMTA1, regulated by Ca^{2+} influx, modulates T cell function in patients with SLE.

Abbreviations

SLE	Systemic lupus erythematosus
NFAT	Nuclear factor of activated T cells (NFAT)
ncRNAs	Noncoding RNAs
lncRNAs	Long ncRNAs
shRNAs	Short ncRNAs
miRNAs	microRNAs
lincRNAs	Long intergenic ncRNAs
asRNAs	antisense RNAs (asRNAs)
circRNAs	circular RNAs
RA	Rheumatoid arthritis
AS	Ankylosing spondylitis
PBMCs	Peripheral blood mononuclear cells
DNMT1	DNA methyltransferase 1
CD	Cluster of differentiation
IL	Interleukin
KLF13	Kruppel-like factor 13
RANTES	Regulated on activation, normal T-cell expressed and secreted
PTPN22	Protein tyrosine phosphatase non-receptor type 22
PMA	Phorbol 12-myristate 13-acetate
IFN-α	Interferon-alpha
LPS	Lipopolysaccharides
RT-PCR	Real-time reverse transcription-polymerase chain reaction
ELISA	Enzyme-linked immunosorbent assay
SDS-PAGE	sodium dodecyl sulfate polyacrylamide gel electrophoresis
PVDF	Polyvinyllidene difluoride
SLEDAI-2K	Systemic Lupus Erythematosus Disease Activity Index 2000
ERCC4	Excision repair cross-complementation group 4
MYH10	Myosin Heavy Chain 10
CAMTA1	Calmodulin Binding Transcription Activator 1
ASH1L	Absent, small, or homeotic1-like
SOCS7	Suppressor of cytokine signaling 7
ASAP1	ArfGAP with SH3 domain, ankyrin repeat and PH domain 1
ASO	Antisense oligonucleotide
PEPCK-M	Mitochondrial phosphoenolpyruvate carboxykinase
TAMs	Tumor-associated macrophages
UTR	Untranslated region

Supplementary Information

The online version contains supplementary material available at https://doi.org/10.1186/s13075-024-03422-6.

Supplementary Material 1

Supplementary Material 2

Supplementary Material 3

Supplementary Material 4

Acknowledgements
We thank Dr. Malcolm Koo for his assistance in manuscript preparation.

Author contributions
H-CY, H-BH, H-Y HT, and M-CL contributed to study design. H-CY, M-CL, H-Y HT and H-BH contributed to experiments, and data analysis. M-CL contributed to patient recruitment and clinical assessment. H-CY, M-CL, and H-BH contributed to manuscript writing. All authors reviewed the manuscript and approved the submitted version.

Funding
This work was supported by grants from the Ministry of Science and Technology (MOST 111-2314-B-303 -007 -MY3) and Buddhist Tzu Chi Medical Foundation (TCMF-A 108-05), Taiwan.

Data availability
NGS data have been uploaded to the Gene Expression Omnibus (GEO) of the National Center for Biotechnology Information and can be accessed at [GEO: GSE278650]. The other data analyzed during the current study are available from the corresponding author on reasonable request.

Declarations

Ethics approval and consent to participate
All the participants signed informed consent under a study protocol approved by the institutional review board of Dalin Tzu Chi Hospital, Buddhist Tzu Chi Medical Foundation (No. B11003006). The study was performed in accordance with the Declaration of Helsinki.

Consent for publication
Not applicable.

Competing interests
The authors declare no competing interests.

Received: 31 July 2024 / Accepted: 21 October 2024
Published online: 29 October 2024

References

1. Tsokos GC. Autoimmunity and organ damage in systemic lupus erythematosus. Nat Immunol. 2020;21:605–14.
2. Moulton VR, Suarez-Fueyo A, Meidan E, Li H, Mizui M, Tsokos GC. Pathogenesis of human systemic lupus erythematosus: a cellular perspective. Trends Mol Med. 2017;23(7):615–35.
3. Kyttaris VC, Wang Y, Juang YT, Weinstein A, Tsokos GC. Increased levels of NF-ATc2 differentially regulate CD154 and IL-2 genes in T cells from patients with systemic lupus erythematosus. J Immunol. 2007;178:1960–6.
4. Liossis SN, Ding XZ, Dennis GJ, Tsokos GC. Altered pattern of TCR/CD3-mediated protein-tyrosyl phosphorylation in T cells from patients with systemic lupus erythematosus. Deficient expression of the T cell receptor zeta chain. J Clin Invest. 1998;101:1448–57.
5. Lu MC, Lai NS, Yu HC, Hsieh SC, Tung CH, Yu CL. Nifedipine suppresses Th1/Th2 cytokine production and increased apoptosis of anti-CD3 + anti-CD28-activated mononuclear cells from patients with systemic lupus erythematosus via calcineurin pathway. Clin Immunol. 2008;129:462–70.
6. Rovin BH, Teng YKO, Ginzler EM, Arriens C, Caster DJ, Romero-Diaz J, et al. Efficacy and safety of voclosporin versus placebo for lupus nephritis (AURORA 1): a double-blind, randomised, multicentre, placebo-controlled, phase 3 trial. Lancet. 2021;397(10289):2070–80.
7. Lai NS, Koo M, Yu CL, Lu MC. Immunopathogenesis of systemic lupus erythematosus and rheumatoid arthritis: the role of aberrant expression of non-coding RNAs in T cells. Clin Exp Immunol. 2017;187:327–36.
8. Chan JJ, Tay Y. Noncoding RNA:RNA regulatory networks in cancer. Int J Mol Sci. 2018;19:1310.
9. Lu MC, Yu HC, Yu CL, Huang HB, Koo M, Tung CH, et al. Increased expression of long noncoding RNAs LOC100652951 and LOC100506036 in T cells from patients with rheumatoid arthritis facilitates the inflammatory responses. Immunol Res. 2016;64:576–83.
10. Yu HC, Huang KY, Lu MC, Huang Tseng HY, Liu SQ, Lai NS, et al. Down-regulation of LOC645166 in T cells of ankylosing spondylitis patients promotes the NF-κB signaling via decreasingly blocking recruitment of the IKK complex to K63-linked polyubiquitin chains. Front Immunol. 2021;12:591706.
11. Wesselhoeft RA, Kowalski PS, Anderson DG. Engineering circular RNA for potent and stable translation in eukaryotic cells. Nat Commun. 2018;9:2629.
12. Zhai X, Zhang Y, Xin S, Cao P, Lu J. Insights into the involvement of circular RNAs in autoimmune diseases. Front Immunol. 2021;12:622316.
13. Wang X, Ma R, Shi W, Wu Z, Shi Y. Emerging roles of circular RNAs in systemic lupus erythematosus. Mol Ther Nucleic Acids. 2021;24:212–22.
14. Liu H, Zou Y, Chen C, Tang Y, Guo J. Current understanding of circular RNAs in systemic lupus erythematosus. Front Immunol. 2021;12:628872.
15. Li LJ, Zhu ZW, Zhao W, Tao SS, Li BZ, Xu SZ, et al. Circular RNA expression profile and potential function of hsa_circ_0045272 in systemic lupus erythematosus. Immunology. 2018;155:137–49.
16. Zhang C, Wang X, Chen Y, Wu Z, Zhang C, Shi W. The down-regulation of hsa_circ_0012919, the sponge for miR-125a-3p, contributes to DNA methylation of CD11a and CD70 in CD4(+) T cells of systemic lupus erythematous. Clin Sci (Lond). 2018;132:2285–98.
17. Jiang Z, Li S, Jia Y, Wu Q, Chen X, Zhang M, et al. CircPTPN22 modulates T-cell activation by sponging miR-4689 to regulate S1PR1 expression in patients with systemic lupus erythematosus. Arthritis Res Ther. 2023;25:206.

18. Lu MC, Yu CL, Chen HC, Yu HC, Huang HB, Lai NS. Aberrant T cell expression of Ca2 + influx-regulated miRNAs in patients with systemic lupus erythematosus promotes lupus pathogenesis. Rheumatology (Oxford). 2015;54:343–8.
19. Hochberg MC. Updating the American College of Rheumatology revised criteria for the classification of systemic lupus erythematosus. Arthritis Rheum. 1997;40:1725.
20. Petri M, Orbai AM, Alarcón GS, Gordon C, Merrill JT, Fortin PR, et al. Derivation and validation of the systemic Lupus International collaborating clinics classification criteria for systemic lupus erythematosus. Arthritis Rheum. 2012;64:2677–86.
21. Gladman DD, Ibañez D, Urowitz MB. Systemic lupus erythematosus disease activity index 2000. J Rheumatol. 2002;29:288–91.
22. Lu MC, Lai NS, Chen HC, Yu HC, Huang KY, Tung CH, et al. Decreased microRNA(miR)-145 and increased miR-224 expression in T cells from patients with systemic lupus erythematosus involved in lupus immunopathogenesis. Clin Exp Immunol. 2013;171:91–9.
23. Yu HC, Huang HB, Huang Tseng HY, Lu MC. Brain-derived neurotrophic factor suppressed proinflammatory cytokines secretion and enhanced microRNA(miR)-3168 expression in macrophages. Int J Mol Sci. 2022;23:570.
24. Zhang J, Chen S, Yang J, Zhao F. Accurate quantification of circular RNAs identifies extensive circular isoform switching events. Nat Commun. 2020;11:90.
25. Wu W, Zhao F, Zhang J. circAtlas 3.0: a gateway to 3 million curated vertebrate circular RNAs based on a standardized nomenclature scheme. Nucleic Acids Res. 2024;52:D52–60.
26. Yu HC, Tung CH, Huang KY, Huang HB, Lu MC. The essential role of peptidylarginine deiminases 2 for cytokines secretion, apoptosis, and cell adhesion in macrophage. Int J Mol Sci. 2020;21:5720.
27. Jitrapakdee S, Walker ME, Wallace JC. Functional expression, purification, and characterization of recombinant human pyruvate carboxylase. Biochem Biophys Res Commun. 1999;266:512–7.
28. Polachek A, Gladman DD, Su J, Urowitz MB. Defining low Disease activity in systemic Lupus Erythematosus. Arthritis Care Res (Hoboken). 2017;69:997–1003.
29. Lietzan AD, St Maurice M. A substrate-induced biotin binding pocket in the carboxyltransferase domain of pyruvate carboxylase. J Biol Chem. 2013;288:19915–25.
30. Jitrapakdee S, St Maurice M, Rayment I, Cleland WW, Wallace JC, Attwood PV. Structure, mechanism and regulation of pyruvate carboxylase. Biochem J. 2008;413:369–87.
31. Liu CX, Li X, Nan F, Jiang S, Gao X, Guo SK et al. Structure and degradation of circular RNAs regulate PKR activation in innate immunity. Cell 2019;177:865–80.
32. Williams BR. Signal integration via PKR. Sci STKE 2001;2001:re2.
33. Trebak M, Kinet JP. Calcium signalling in T cells. Nat Rev Immunol. 2019;19:154–69.
34. Chen X, Song Y, Chen G, Zhang B, Bai Y, Sun C, et al. Circular RNA circFOXO3 functions as a competitive endogenous RNA for acid-sensing ion channel subunit 1 mediating oxeiptosis in nucleus pulposus. Biomedicines. 2024;12:678.
35. Song L, Wang Y, Feng Y, Peng H, Wang C, Duan J, et al. Bioinformatics-based identification of circRNA-microRNA-mRNA network for calcific aortic valve disease. Genet Res (Camb). 2023;2023:8194338.
36. Lieberman LA, Tsokos GC. The IL-2 defect in systemic lupus erythematosus disease has an expansive effect on host immunity. J Biomed Biotechnol. 2010;2010:740619.
37. He J, Zhang R, Shao M, Zhao X, Miao M, Chen J, et al. Efficacy and safety of low-dose IL-2 in the treatment of systemic lupus erythematosus: a randomised, double-blind, placebo-controlled trial. Ann Rheum Dis. 2020;79:141–9.
38. Freen-van Heeren JJ. Post-transcriptional control of T-cell cytokine production: implications for cancer therapy. Immunology. 2021;164:57–72.
39. Xue Q, Guo ZY, Li W, Wen WH, Meng YL, Jia LT, Wang J, Yao LB, Jin BQ, Wang T, Yang AG. Human activated CD4(+) T lymphocytes increase IL-2 expression by downregulating microRNA-181c. Mol Immunol. 2011;48:592–9.
40. Cheng L, Hu S, Ma J, Shu Y, Chen Y, Zhang B, et al. Long noncoding RNA RP11-241J12.3 targeting pyruvate carboxylase promotes hepatocellular carcinoma aggressiveness by disrupting pyruvate metabolism and the DNA mismatch repair system. Mol Biomed. 2022;3:4.
41. Cappel DA, Deja S, Duarte JAG, Kucejova B, Iñigo M, Fletcher JA et al. Pyruvate-carboxylase-mediated anaplerosis promotes antioxidant capacity by sustaining TCA cycle and redox metabolism in liver. Cell Metab 2019;29:1291–305.
42. Shah A, Wondisford FE. Gluconeogenesis flux in metabolic disease. Annu Rev Nutr. 2023;43:153–77.
43. Méndez-Lucas A, Hyroššová P, Novellasdemunt L, Viñals F, Perales JC. Mitochondrial phosphoenolpyruvate carboxykinase (PEPCK-M) is a pro-survival, endoplasmic reticulum (ER) stress response gene involved in tumor cell adaptation to nutrient availability. J Biol Chem. 2014;289:22090–102.
44. Baker R, Hontecillas R, Tubau-Juni N, Leber AJ, Kale S, Bassaganya-Riera J. Computational modeling of complex bioenergetic mechanisms that modulate CD4 + T cell effector and regulatory functions. NPJ Syst Biol Appl. 2022;8:45.
45. Li H, Boulougoura A, Endo Y, Tsokos GC. Abnormalities of T cells in systemic lupus erythematosus: new insights in pathogenesis and therapeutic strategies. J Autoimmun. 2022;132:102870.
46. Yin Y, Choi SC, Xu Z, Zeumer L, Kanda N, Croker BP, et al. Glucose oxidation is critical for CD4 + T cell activation in a mouse model of systemic lupus erythematosus. J Immunol. 2016;196:80–90.
47. Shu Y, Yang N, Cheng N, Zou Z, Zhang W, Bei Y, et al. Intervening pyruvate carboxylase stunts tumor growth by strengthening anti-tumor actions of tumor-associated macrophages. Signal Transduct Target Ther. 2022;7:34.
48. Liang QH, Li QR, Chen Z, Lv LJ, Lin Y, Jiang HL, et al. Anemoside B4, a new pyruvate carboxylase inhibitor, alleviates colitis by reprogramming macrophage function. Inflamm Res. 2024;73:345–62.
49. Tanaka Y, Kusuda M, Yamaguchi Y. Interferons and systemic lupus erythematosus: Pathogenesis, clinical features, and treatments in interferon-driven disease. Mod Rheumatol. 2023;33:857–67.
50. Mathian A, Mouries-Martin S, Dorgham K, Devilliers H, Yssel H, Garrido Castillo L, et al. Ultrasensitive serum interferon-α quantification during SLE remission identifies patients at risk for relapse. Ann Rheum Dis. 2019;78:1669–76.
51. Morand EF, Furie R, Tanaka Y, Bruce IN, Askanase AD, Richez C, et al. Trial of anifrolumab in active systemic lupus erythematosus. N Engl J Med. 2020;382:211–21.

Publisher's note